Parton-to-Kaon Fragmentation Revisited

Daniel de Florian
International Center for Advanced Studies (ICAS), UNSAM, Campus Miguelete, 25 de Mayo y Francia (1650) Buenos Aires, Argentina

Manuel Epele
Instituto de Física La Plata, CONICET - UNLP, Departamento de Física, Facultad de Ciencias Exactas, Universidad de La Plata, C.C. 69, La Plata, Argentina

Roger J. Hernández-Pinto
Facultad de Ciencias Físico-Matemáticas, Universidad Autónoma de Sinaloa, Ciudad Universitaria, CP80000, Culiacán, Sinalo, México

R. Sassot
Departamento de Física and IFIBA, Facultad de Ciencias Exactas y Naturales, Universidad de Buenos Aires, Ciudad Universitaria, Pabellón 1 (1428) Buenos Aires, Argentina

Marco Stratmann
Institute for Theoretical Physics, University of Tübingen, Auf der Morgenstelle 14, 72076 Tübingen, Germany

We revisit the global QCD analysis of parton-to-kaon fragmentation functions at next-to-leading order accuracy using the latest experimental information on single-inclusive kaon production in electron-positron annihilation, lepton-nucleon deep-inelastic scattering, and proton-proton collisions. An excellent description of all data sets is achieved, and the remaining uncertainties in parton-to-kaon fragmentation functions are estimated and discussed based on the Hessian method. Extensive comparisons to the results from our previous global analysis are made.

PACS numbers: 13.87.Fh, 13.85.Ni, 12.38.Bx

I. INTRODUCTION AND MOTIVATION

Parton-to-hadron fragmentation functions (FFs) parametrize how quarks and gluons that are produced in hard interactions at high energies confine themselves into hadrons measured and identified in experiment [1]. This information is beyond the reach of perturbative Quantum Chromodynamics (pQCD) and must therefore be inferred from the wealth of data on identified hadron production under the theoretical assumption that the relevant non-perturbative dynamics of FFs factorizes in a universal way from the calculable hard partonic cross sections [2] up to small corrections which can be usually neglected.

A precise knowledge on FFs is vital for the quantitative description of a wide variety of hard scattering processes designed to probe the spin and flavor structure of nucleons and nuclear matter and their interpretation at the most elementary and fundamental level. Even though the role of FFs has been highlighted since the early days of the parton model [1], only relatively recently it has become possible to combine precise enough data from different processes with perturbative calculations of matching accuracy to determine FFs for identified pions and kaons within meaningful uncertainties in what is now commonly known as the "DSS 07 global analysis" [3].

Precise parton-to-kaon FFs are usually considered as a key ingredient to probe the strangeness content of the nucleon and are expected to be of crucial importance in further constraining the corresponding momentum distributions at a future Electron-Ion Collider (EIC) through charged kaon production in semi-inclusive deep-inelastic scattering (SIDIS) [4]. This is especially the case for the helicity-dependent strangeness parton distributions Δs and $\Delta\bar{s}$ [5, 6], largely because of the complete lack of other experimental constraints from neutrino-induced, electroweak deep-inelastic structure function measurements [7] that are routinely utilized in all extractions of unpolarized parton distribution functions (PDFs), see, e.g., [8–10]. For the discussions below, it should be kept in mind that the unpolarized strangeness PDF is also less well constrained than the light sea quarks, see, e.g., [8].

The relatively poor precision achieved for the available parton-to-kaon FFs [3, 11] is an important limiting factor, with relative uncertainties roughly one order of magnitude larger than those estimated for the corresponding parton-to-pion FFs [3, 12]. This is readily understood from the fact that pions are much more copiously produced and easier to identify experimentally than kaons and that their perturbative description is not so much challenged by potentially large kinematical corrections associated with the hadron's mass that is usually neglected in the underlying theoretical framework [13]. The lack of precision for kaon FFs has, for instance, led

to quite some discussions [14] concerning the smallish Δs obtained in the analysis of kaon production in polarized SIDIS [5], a question that can likely only be settled in the future at an EIC by more precise SIDIS measurements in a broader kinematic range along with an improved theoretical analysis based on more reliable kaon FFs.

Since the DSS 07 analysis [3], still the only global QCD analysis of kaon FFs available, strenuous efforts have been made to produce considerably more precise data on inclusive hadron production. In Ref. [15], we performed an update of the DSS 07 results for pion FFs (DSS 14), including all the newly available sets of data at that time. In addition, an iterative Hessian (IH) approach was implemented to assess the uncertainties [16] and to provide Hessian uncertainty sets to facility propagating uncertainties related to FFs to any process of interest. In what follows, we revisit also our previous global analysis of kaon FFs and perform similar updates to the latest sets of experimental data and to the way uncertainties are estimated.

More specifically, including single-inclusive electron-positron annihilation (SIA) data from BaBar [17] and Belle [18] should, in principle, provide a better handle on the gluon-to-kaon FF through QCD scaling violations of the SIA structure functions between the scale $Q = M_Z$, relevant for the LEP and SLAC experiments included in DSS 07, and the scale corresponding to the center-of-mass system (c.m.s.) energy of BaBar and Belle, $Q = \sqrt{S} \simeq 10.5\,\text{GeV}$. In addition, since the electroweak couplings of up-type and down-type quarks to the Z boson become almost equal at $Q \approx M_Z$, LEP and SLAC data are mainly sensitive to the total quark singlet FF for any observed hadron H. At the lower $\sqrt{S}$ of BaBar and Belle, the quark-antiquark pairs in SIA are produced according to their electrical charge, which, in our global fit, should allow for some partial flavor separation of kaon FFs.

Another important and new ingredient to the current global analysis is the final SIDIS data for proton and deuteron targets released by the Hermes Collaboration [19], which supersede the preliminary data [20] utilized (only for proton targets) in the DSS 07 fit. This time, we include both the $z - Q^2$ and $z - x$ projections of the multi-dimensional Hermes multiplicities, at variance with DSS 07 where only the $z - Q^2$ projections were considered. Since most of the events [O(70%)] in either of the two projections are not shared [21], both sets provide highly valuable information worth including in the fit. In addition, since the different bins in x involve combinations of the FFs weighted by significantly different PDFs, the $z - x$ projections are expected to lead to a much tighter constraint on the flavor separation than the $z - Q^2$ projections alone, where this information is integrated out and potentially diluted. We also pay special attention to the kinematical dependence of the SIDIS cross sections within each bin, and integrate these contributions rather than computing the cross sections at the mean kinematical values as quoted by the experiment, which may lead to significant differences for the estimated multiplicity values [21].

Another crucial addition to the available suite of data on identified charged kaons are first multiplicity results in SIDIS from the Compass experiment at CERN [22]. These data are very precise despite exhibiting a rather fine binning in the relevant kinematic variables. Most importantly, Compass multiplicities reach much higher values of momentum transfer $Q^2 \lesssim 60\,\text{GeV}^2$ than Hermes $Q^2 \lesssim 30\,\text{GeV}^2$ and, therefore, combining them in a global fit not only allows us to test and quantify their level of consistency, but should, in principle, also lead to a considerably better flavor separation of the obtained parton-to-kaon FFs. Not surprisingly, the largest differences with respect to the original DSS 07 analysis are found mainly at the higher Q^2 values not covered by the Hermes data.

Finally, first results on single-inclusive kaon spectra at high transverse momenta p_T have become available from the LHC at c.m.s. energies of up to 2.76 TeV [23], which nicely supplement the data from BNL-RHIC taken at $\sqrt{S} = 200\,\text{GeV}$ that have been already used in the original DSS 07 analysis. Here, we also include new results from the Star Collaboration for charged kaon production at $\sqrt{S} = 200\,\text{GeV}$ [24].

The main goal of our new analysis is to extract an updated, more precise set of parton-to-kaon FFs and to determine their uncertainties reliably based on the IH method [16] in light of all the newly available experimental results in SIA, SIDIS, and pp collisions. This will allow us to scrutinize the consistency of the information on FFs extracted across the different hard scattering processes, i.e., to validate the fundamental notion of universality, which is at the heart of any pQCD calculation based on the factorization of short- and long-distance physics [2] mentioned at the beginning. Since extractions of leading order (LO) FFs have yielded a much less satisfactory description of the available pion production data in the past [3], we only perform our global QCD fit at next-to-leading order (NLO) accuracy. We note, that first efforts have started recently to perform extractions of pion FFs from SIA data at next-to-next-to-leading order (NNLO) accuracy [25] or even by including all-order resummations [26]. Since the relevant cross sections for SIDIS and pp collisions are not yet available at NNLO accuracy, a global QCD analysis of FFs can be consistently performed only at the NLO level for the time being.

The remainder of the paper is organized as follows: in the next section, we briefly summarize the main aspects of our updated global analysis, including the choice of the functional form used to parametrize the FFs at the initial scale Q_0 for the QCD evolution, the selection of data sets and the cuts imposed on them, and the treatment of experimental normalization uncertainties. The outcome of the new fit is discussed in depth in Sec. III. The obtained parton-to-kaon fragmentation functions and their uncertainties are shown and compared to the results of our previous global analysis. Detailed comparisons to the

individual data sets are given to demonstrate the quality of the fit. Potential open issues and tensions among the different data sets will be discussed. We briefly summarize the main results in Sec. IV.

II. TECHNICAL FRAMEWORK

Since the main features and technical details of our global QCD extractions of FFs for various types of identified hadrons have already been discussed at length in the literature [3, 12, 15, 27, 28], we mainly focus in the following on those aspects that differ from the original DSS 07 analysis of parton-to-kaon FFs [3].

A. Functional Form and Fit Parameters

As in the case of our updated pion FFs in Ref. [15], the functional form adopted in the original DSS 07 global analysis [3] is still flexible enough to accommodate also the wealth of new experimental information included in the present fit. Therefore, we continue to parametrize the hadronization of a parton of flavor i into a positively charged kaon K^+ at an initial scale of $Q_0 = 1\,\mathrm{GeV}$ as

$$D_i^{K^+}(z,Q_0) = \frac{N_i\, z^{\alpha_i}(1-z)^{\beta_i}[1+\gamma_i(1-z)^{\delta_i}]}{B[2+\alpha_i,\beta_i+1]+\gamma_i B[2+\alpha_i,\beta_i+\delta_i+1]}\,. \tag{1}$$

Here, $B[a,b]$ denotes the Euler Beta-function, and the N_i in (1) are chosen in such a way that they represent the contribution of $zD_i^{K^+}$ to the momentum sum rule. z is the fraction of momentum of the parton i taken by the kaon. As in our previous analysis [3], we fit $D_{u+\bar{u}}^{K^+}$ and $D_{s+\bar{s}}^{K^+}$, containing the "valence" quarks in a K^+ meson, independently, but use a single parameterization for all the unfavored quark flavors since the data are still unable to discriminate between them. Different flavor-breaking scenarios have been explored, but they do not change the quality of the fit or even lead to a poor convergence of the fit due to the extra parameters that need to be introduced. However, the improved experimental information available in the present fit now allows us to impose less constraints on the parameter space spanned by the input function in Eq. (1). Specifically, in Ref. [3] some parameters had to be set to fixed values from the start, whereas now all the parameters can exploit a greater degree of flexibility in the fit and, in principle, can be determined by data. Of course, one always has to ensure proper convergence of the fit and, since we are interested in Hessian uncertainty sets, avoid any parameters that are only very weakly constrained. Specifically, it turns out that $\beta_g \simeq \beta_{\bar{u}}$, $\gamma_{s+\bar{s}} \simeq \gamma_{\bar{u}}$, and $\delta_{s+\bar{s}} \simeq \delta_{\bar{u}}$, such that we decided to identify these parameters with each other without any change in the total χ^2 of the fit.

No new charm or bottom-tagged data in SIA have become available since the DSS 07 analysis but the new, very precise results from BaBar [17] and Belle [18] in SIA and from Compass [22] and Hermes [19] in SIDIS now constrain both the total quark singlet fragmentation function, i.e., summed over all flavors, and the individual, flavor-separated light quark FFs much better than before. Nevertheless, it turns out that the charm- and bottom-to-kaon FFs can still accommodate these changes with $\gamma_{c+\bar{c}} = \gamma_{b+\bar{b}} \simeq 0$ such that we can identify these parameters with zero. In addition, one can set $\alpha_{c+\bar{c}} = \alpha_{b+\bar{b}}$ without any change to the fit. As in the DSS 07 and other analyses of FFs, we include heavy flavor FFs discontinuously as massless partons in the QCD scale evolution above their $\overline{\mathrm{MS}}$-scheme "thresholds", $Q = m_{c,b}$, with m_c and m_b denoting the mass of the charm and bottom quark, respectively. We note, that the effects of accounting for heavy quark masses in extracting light hadron FFs have been explored recently in the case of pion FFs with interesting results [29]. For the time being, and to allow for a comparison to our previous results from the DSS 07 fit, we restrict ourselves in the current analysis to the usually adopted "zero-mass variable flavor number approximation".

In total we now have 20 free fit parameters describing our updated FFs for quarks, antiquarks, and gluons into a positively charged kaon. They are determined from data by a standard χ^2-minimization procedure that includes a χ^2-penalty from computing the optimum relative normalization of each experimental set of data analytically as was outlined in the DSS 14 analysis of pion FFs [15]. The latter treatment is at variance with the DSS 07 analysis, where the data sets were allowed to float without any χ^2-penalty within the quoted normalization uncertainties. The corresponding FFs for negatively charged kaons are obtained, as usual, by charge conjugation symmetry.

B. Data Selection

In addition to the data sets already used in the DSS 07 global analysis [3], we now utilize the new results from BaBar [17] and Belle [18] in SIA at a c.m.s. energy of $\sqrt{S} \simeq 10.5\,\mathrm{GeV}$. Both sets are very precise and reach all the way up to kaon momentum fractions z close to one, well beyond of what has been covered so far by SIA data. We analyze both sets with $n_f = 4$ active, massless flavors using the standard expression for the SIA cross section at NLO accuracy. As is customary, we limit ourselves to data with $z \geq 0.1$ to avoid any potential impact from kinematical regions where finite, but neglected, hadron mass corrections, proportional to $M_K/(Sz^2)$, might become of any importance. Since mass effects grow considerably at lower $\sqrt{S}$ we only use data from BaBar with $z \geq 0.2$; there are no Belle data below that cut. For all previous SIA data, taken at higher $\sqrt{S}$, we use $n_f = 5$ and also $z \geq 0.1$, following the original DSS 07 analysis. Any incompatibility of the two new, precise sets of data at $\sqrt{S} \simeq 10.5\,\mathrm{GeV}$ with each other or with the old LEP and SLAC data at $\sqrt{S} \simeq 91.2\,\mathrm{GeV}$ [30–33] has the

potential to seriously spoil the quality of the global fit.

In case of SIDIS, we replace the preliminary multiplicity data from HERMES [20] by their final results [19]. More specifically, we use the data for charged kaon multiplicities in four bins of z as a function of both momentum transfer Q^2 and the target nucleon's (proton or deuteron) momentum fraction x. The kinematical ranges of average values of Q^2 and x covered by these data are from about $1.1\,\mathrm{GeV}^2$ to $7.4\,\mathrm{GeV}^2$ and 0.064 to 0.277, respectively, for the $z-Q^2$ projections and from about $1.19\,\mathrm{GeV}^2$ to $10.24\,\mathrm{GeV}^2$ and 0.034 to 0.45, respectively, for the $z-x$ projections, with $0.2 \leq z \leq 0.8$. Most of the events, O(70%), in either of the two projections are not shared [21].

In addition, we include for the first time multiplicity data for $K^{\pm}$ production from the COMPASS Collaboration [22], which are given as a function of z in bins of inelasticity y (i.e. Q^2) and the initial-state momentum fraction x. The coverage in z is the same as for the HERMES data, but due to the higher $\sqrt{S}$ of the COMPASS experiment, the reach in x and Q^2 is significantly broader. Experimental information is available for $0.004 \leq x \leq 0.7$ and $1.2 \leq Q^2 \leq 60\,\mathrm{GeV}^2$. It turns out, that we do not have to impose any cuts on both data sets to accommodate them in the global analysis. As for the SIA data, having now available two precise sets of multiplicity data in SIDIS, covering somewhat different but partially overlapping kinematics, makes it very important to validate their consistency in a global fit.

Finally, we update and add new sets of data for inclusive high-p_T kaon production in pp collisions with respect to those included in the DSS 07 analysis. Most noteworthy are the first results for the kaon-to-pion ratio from the ALICE Collaboration at CERN-LHC [23], covering unprecedented c.m.s. energies of up to 2.76 TeV. In addition, we include STAR data taken at $\sqrt{S} = 200\,\mathrm{GeV}$ for charged kaon production and for the K^-/K^+ ratio [24]. As was discussed in detail in Ref. [15] in the context of pion FFs, it turns out that a good global fit of RHIC and LHC pp data, along with all the other world data, can only be achieved if one imposes a cut on the minimum p_T of the produced hadron of about 5 GeV. We maintain this cut also for the present global analysis, but we will illustrate how the obtained fit extrapolates to data at lower values of p_T. Such a p_T-cut eliminates all the old pp data sets included in the previous DSS 07 analysis from the fit, specifically, the BRAHMS [35] and the STAR [36] data.

In Tab. I, we list all data sets included in our global analysis along with the individual χ^2 values obtained in the fit, to which we now turn.

TABLE I: Data sets used in our NLO global analysis, their optimum normalization shifts N_i, the individual χ^2 values (including the χ^2 penalty from the obtained N_i), and the total χ^2 of the fit. In case of SIDIS, we denote the charge $K^{\pm}$, the target hadron (p) or (d), and, for HERMES, also the data projection $z-Q^2$ and $z-x$ as Q^2 and x, respectively.

experiment	data type	norm. N_i	# data in fit	χ^2
TPC [37]	incl.	1.003	12	13.4
SLD [33]	incl.	1.014	18	17.2
	uds tag	1.014	10	31.5
	c tag	1.014	10	21.3
	b tag	1.014	10	11.9
ALEPH [30]	incl.	1.026	13	29.7
DELPHI [31]	incl.	1.000	12	6.9
	uds tag	1.000	12	13.1
	b tag	1.000	12	11.0
OPAL [34]	u tag	0.778	5	9.6
	d tag	0.778	5	7.7
	s tag	0.778	5	23.4
	c tag	0.778	5	42.5
	b tag	0.778	5	16.9
BABAR [17]	incl.	1.077	45	30.6
BELLE [18]	incl.	0.996	78	15.6
HERMES [19]	K^+ (p) Q^2	0.843	36	61.9
	K^- (p) Q^2	0.843	36	29.6
	K^+ (p) x	1.135	36	75.8
	K^- (p) x	1.135	36	42.1
	K^+ (d) Q^2	0.845	36	44.7
	K^- (d) Q^2	0.845	36	41.9
	K^+ (d) x	1.095	36	48.9
	K^- (d) x	1.095	36	44.4
COMPASS [22]	K^+ (d)	0.996	309	285.8
	K^- (d)	0.996	309	265.1
STAR [24]	K^+,K^-/K^+	1.088	16	7.6
ALICE [23] 2.76 TeV	K/π	0.985	15	21.6
TOTAL:			1194	1271.7

III. RESULTS

In this section we present and discuss in depth the results of our global analysis of parton-to-kaon FFs. First, we present the optimum fit parameters, normalization shifts, and the individual χ^2 values of each data set. Next, the newly obtained $D_i^{K^+}(z,Q^2)$ and their uncertainty estimates are shown and compared to the results of the previous DSS 07 fit. The quality of the fit to SIA, SIDIS, and pp data and potential open issues and tensions among the different sets of data are illustrated and discussed in Secs. III B, III C, and III D, respectively.

A. Parton-To-Kaon Fragmentation Functions

In Table II we list the obtained set of parameters in Eq. (1) specifying our updated, optimum parton-to-kaon fragmentation functions at NLO accuracy at the input scale $Q_0 = 1\,\mathrm{GeV}$ for the light quark flavors and the gluon, and for the charm and bottom quarks at their respective mass thresholds $Q_0 = m_{c,b}$. The new NLO FFs $D_i^{K^+}(z,Q^2)$, evolved to two different values of Q^2, are shown as a function of z in Figs. 1 and 2 along with our estimates of uncertainties at both 68% and 90% confidence

TABLE II: Parameters describing the NLO FFs for positively charged kaons, $D_i^{K^+}(z,Q_0)$, in Eq. (1) in the $\overline{\rm MS}$ scheme at the input scale $Q_0 = 1\,{\rm GeV}$. Results for the charm and bottom FFs refer to $Q_0 = m_c = 1.43\,{\rm GeV}$ and $Q_0 = m_b = 4.3\,{\rm GeV}$, respectively.

flavor i	N_i	α_i	β_i	γ_i	δ_i
$u+\overline{u}$	0.0663	-0.486	0.098	10.85	1.826
$s+\overline{s}$	0.2319	2.745	2.867	59.07	7.421
$\overline{u}=d=\overline{d}=s$	0.0059	3.657	12.62	59.07	7.409
$c+\overline{c}$	0.1255	-0.941	2.145	0.0	0.0
$b+\overline{b}$	0.0643	-0.941	5.221	0.0	0.0
g	0.0283	13.60	12.62	0.0	0.0

level (C.L.) and the results from our previous DSS 07 fit [3]. As can be inferred from the figures, the FFs for most flavors are either close to the updated fit or within its 90% C.L. uncertainty band; one should recall, that only data with $z \geq 0.1$ are included in our analysis [$z \geq 0.2$ for BABAR]. For some flavors i and regions of z there are, however, sizable differences. They are most noticeable for $D_{u+\bar{u}}^{K^+}$ and the unfavored FF $D_{\bar{u}}^{K^+}$ below $z \simeq 0.5$, for $D_{c+\bar{c}}^{K^+}$ at large z, and for the gluon-to-kaon FF around $z \simeq 0.4$.

The differences with respect to the DSS 07 results are mainly driven by the newly added BELLE and BABAR data at high z, by the $z-x$ projections of the multiplicities both from HERMES [19] and COMPASS [22], and by the K^-/K^+ ratios measured in pp collisions by STAR [24]. All these sets provide sensitivity to the flavor separation of the parton-to-kaon FFs that was not available in the DSS 07 analysis, and in the global fit all FFs have to adjust accordingly. It is worth noticing that the total strange quark FF $D_{s+\bar{s}}^{K^+}$, which plays an important role in determinations of the strangeness helicity distribution [5], is always somewhat smaller than the corresponding DSS 07 result, but the differences are within the 90% C.L. uncertainty band for $z \gtrsim 0.1$. In spite of the much improved experimental information, no evidence of a flavor symmetry breaking between the unfavored FFs is found. A single parameterization for $D_{\bar{u}}^{K^+} = D_d^{K^+} = D_{\bar{d}}^{K^+} = D_s^{K^+}$ is still the most economical choice to reproduce the data, as was the case in the original DSS 07 analysis.

In terms of uncertainties, the strange quark FF is less well constrained than other FFs despite being a "favored" FF. Light quark FFs have the advantage that u and d quarks are much more abundant than s quarks in SIDIS due to the corresponding u and d valence quark PDFs. In addition, scattering off a u-quark is more likely due to its larger electrical charge. The heavy quark FFs are rather tightly constrained by flavor-tagged SIA data and, thanks to the new BELLE and BABAR data, to some extent also from their interplay with LEP and SLAC data at higher c.m.s. energies; for instance, for BELLE and BABAR the bottom FFs does not play a role.

The overall quality of the fit is summarized in Tab. I,

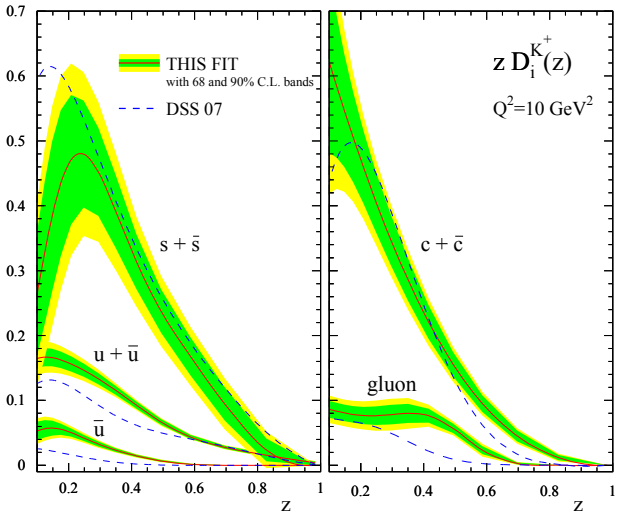

FIG. 1: The individual FFs for positively charged kaons $zD_i^{K^+}(z,Q^2)$ at $Q^2 = 10\,{\rm GeV}^2$ (solid lines) along with uncertainty estimates at 68% and 90% C.L. indicated by the inner and outer shaded bands, respectively. Also shown is a comparison to our previous DSS 07 global analysis [3] (dashed lines).

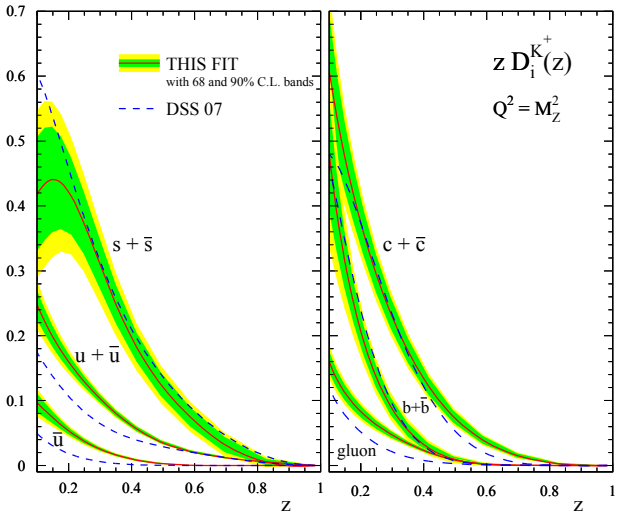

FIG. 2: As in Fig. 1 but now at the scale $Q = M_Z$ where also the bottom-to-K^+ fragmentation function is nonzero.

where we list all data sets included in our global analysis, as discussed in Sec. II B, along with their individual χ^2 values and the analytically determined normalization shifts for each set. We note that the quoted χ^2 values are based only on fitted data points, i.e., after applying the cuts mentioned in Sec. II B, and include the χ^2 penalty from the normalization shifts; see Ref. [15] for more details on the method.

It is also worth mentioning that there is a more than five-fold increase in the number of available data points

as compared to the original DSS 07 analysis [3]. Secondly, the overall quality of the global fit has improved dramatically from χ^2/d.o.f. $\simeq 1.83$ for DSS 07, see Tab. V in Ref. [3], to χ^2/d.o.f. $\simeq 1.08$ for the current fit. A more detailed inspection reveals that the individual χ^2 values for the SIA data [30–33, 37], which were already included in the DSS 07 fit, have, by and large, not changed significantly. The biggest improvement concerns the SIDIS multiplicities from HERMES which, in their published version [19], are described rather well by the updated fit, with only a few exceptions; see below. Also, the charged kaon multiplicities from COMPASS [22] and the new SIA data from BABAR [17] and BELLE [18] integrate very nicely into the global QCD analysis of parton-to-kaon FFs at NLO accuracy. We recall that the original DSS 07 fit was based on the 2003 NLO (2002 LO) PDF set [38] ([39]) from the MRST group. In the present fit, the underlying set of PDFs has have been upgraded to the recent MMHT 2014 analysis [9], that gives a much more accurate description of sea-quark parton densities on which the analysis of SIDIS multiplicities depends rather strongly. We have checked that very similar results for kaon FFs are obtained with other up-to-date sets of PDFs such as [8, 10]. Nevertheless, the corresponding PDF uncertainty is included in the χ^2-minimization procedure and, hence, the quoted χ^2 values for SIDIS multiplicities.

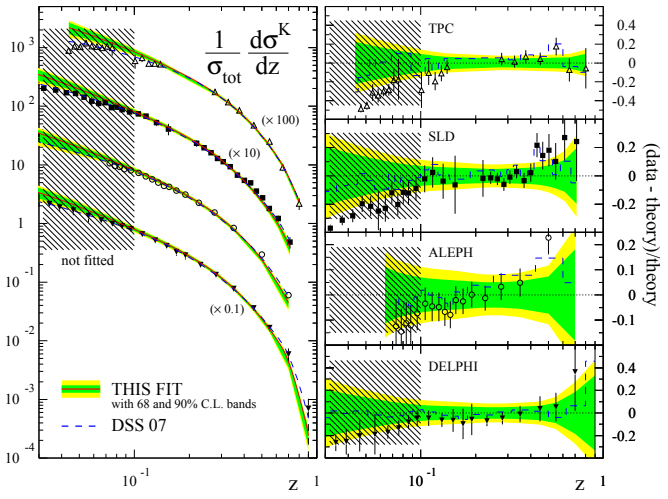

FIG. 3: Left-hand side: comparison of our new NLO results (solid lines) and the previous DSS 07 fit [3] (dashed lines) with data sets for inclusive kaon production in SIA used in both fits, see Tab. I. The inner and outer shaded bands correspond to new uncertainty estimates at 68% and 90% C.L., respectively. Right-hand side: "(data-theory)/theory" for each of the data sets w.r.t. our new fit (symbols) and the DSS 07 analysis (dashed lines).

B. Electron-Position Annihilation Data

In Figs. 3 and 4 we present a detailed comparison of the results of our fit and its uncertainties at both 68% and 90% C.L. with the SIA data already included and newly added to the original DSS 07 analysis [3], respectively. In general, the agreement of the fit with SIA data is excellent in the entire energy and z-range covered by the experiments. The new fit reproduces SLAC and LEP data at $Q = M_Z$ as well or even slightly better than the old DSS 07 result for $z \geq 0.1$, and improves very significantly the description of the newly added BELLE and BABAR data as can be best seen from the "(data-theory)/theory" panels in Fig. 4; recall that only data with $z \geq 0.2$ are included in the fit for BABAR due the lower $\sqrt{S}$. This is mainly achieved by changing the singlet flavor combinations rather significantly at large $z \sim 0.5 - 0.8$ at the lower Q relevant for BELLE and BABAR. For SIA data at z-values lower than those included in the χ^2 minimization, the old DSS 07 fit gives, however, a better description when extrapolated, presumably because the fit has to accommodate much less data.

The BELLE data [18], shown in Fig. 4, provide not only the finest binning in z but also reach the highest z-values measured so far. Above $z \gtrsim 0.8$ one observes an increasing trend for the new fit to overshoot the data, still within the estimated and growing theoretical (and experimental) uncertainties though. In this kinematic regime one expects large logarithmic corrections, which appear

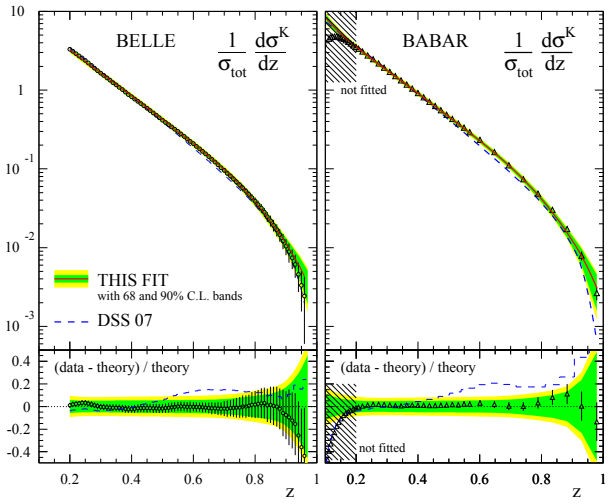

FIG. 4: Left-hand side: comparison of our new NLO results (solid line) with the new BELLE data [18]; also shown is the result obtained with the DSS 07 fit [3] (dashed line). Right-hand side: same, but now for the BABAR data [17]. Lower panels: "(data-theory)/theory" for each of the data sets w.r.t. our new fit (symbols) and the DSS 07 analysis (dashed lines). The inner and outer shaded bands correspond to the new uncertainty estimates at 68% and 90% C.L., respectively. Data below $z = 0.2$ are not included in the fit.

in each order of perturbation theory, to become more and more relevant. It is known how to resum such terms to

all orders in the strong coupling [40], and it might be worthwhile to explore their relevance and whether they could further improve the agreement with data in a future dedicated analysis in detail. Resummations also provide a window to non-perturbative contributions to the perturbative series so far little explored. The z-binning of BABAR data [17] is more sparse towards large z, and a similar trend as for the BELLE data is not visible here.

Our estimated uncertainty bands at 68% and 90% C.L. are also shown in Figs. 3 and 4. They reflect the accuracy and kinematical coverage of the fitted data sets and, hence, increase towards both small and large values of z, very similar to the pattern observed for the individual FFs $D_i^{K^+}$ in Figs. 1 and 2. One should keep in mind, however, that the obtained bands are constrained by the fit to the *global* set of SIA, SIDIS, and *pp* data and do not necessarily have to follow the accuracy of each *individual* set of data.

Turning again to the extrapolation of the new fit to data below the cut of $z = 0.1$ ($z = 0.2$ for BABAR), one can infer from Figs. 3 and 4 that the NLO theory estimates continue to rise while the data start to drop towards lower values of z for all sets. Such an effect is not unexpected and signifies the onset of neglected hadron mass effects in the theoretical framework. In fact, this is, in general, the very reason for all fits of FFs to SIA data to choose some lower cut on z. Due to the higher mass of the kaons, we decided to impose also a slightly higher cut of $z \geq 0.1$ than what was used for pions in the latest DSS 14 analysis [15]. Another issue with the small-z region has to do with strongly enhanced terms in the perturbative series of both the time-like splitting functions and the SIA coefficient functions that become more and more severe in higher orders and would require the use of all-order resummation techniques [26].

C. Semi-Inclusive DIS Multiplicities

The most powerful constraint for flavor-separated FFs comes from charged kaon multiplicities in SIDIS. Contrary to SIA, which produces K^+ and K^- at equal rates, SIDIS multiplicities are sensitive to the produced hadron's charge, through the choice of the target hadron and the kinematics, i.e., the parton momentum fraction x that is probed. For instance, data taken on a proton target in the valence region (medium-to-large values of x) will contain more K^+ than K^- mesons, since u-quarks are much more abundant in a proton than $\bar{u}$-quarks. The access to precisely measured multiplicities for positively and negatively charged kaons, produced alternatively off proton or deuteron targets, and within different regions of proton momentum fractions x allows for studying the flavor dependence of parton-to-kaon FFs at an unprecedented level of accuracy.

Compared with the DSS 07 analysis, where we only had some preliminary set of kaon multiplicities on a proton target from the HERMES Collaboration at our disposal [20], we can now use their published, final set of data for both proton and deuteron targets [19]. In Fig. 5 we illustrate the quality of the new fit with respect to the HERMES data. Shown are the charged kaon multiplicities $M_{e,p(d)}^{K^\pm}$, which are defined as the ratio of the inclusive kaon yield and the total DIS cross section in the same x and Q^2 bin in lepton-proton (lp) or lepton-deuteron (ld) scattering:

$$M_{l,p(d)}^{K^\pm} \equiv \frac{d\sigma_{l,p(d)}^{K^\pm}/dx\,dQ^2\,dz}{d\sigma_{l,p(d)}/dx\,dQ^2}\,. \tag{2}$$

In the global fit we consider the two-dimensional projections of the three-dimensional multiplicity data [19] onto the $z-Q^2$ dependence (left-hand-side of Fig. 5) and, for the first time, also the $z-x$ dependence (right-hand-side), for four different bins of the kaon's momentum fraction z. The interplay of these data, i.e., the attempt to fit them both simultaneously, provides a much improved sensitivity to the flavor-structure of the parton-to-kaon FFs. As was mentioned in the Introduction and noticed in Ref. [21], we find it important to carefully include the full kinematic dependence of the SIDIS cross section by integrating within the boundaries of each bin rather than simply adopting the quoted mean values for x, Q^2, and z.

The actual extraction of the FFs from SIDIS multiplicities receives a further complication from the need to choose a certain set of non-perturbative PDFs for the proton (deuteron) target which also need to be obtained from global QCD analyses to data; see, for instance, Refs. [8–10]. Much progress has been made in recent years in carefully quantifying and reducing the uncertainties of PDFs, thanks to the high demand for precise theoretical estimates for the CERN-LHC program. Here, and for the analyses of *pp* data below, we adopt the recent set by the MMHT 2014 group [9], along with their Hessian uncertainty sets to properly propagate PDF uncertainties to our extraction of FFs, see below. We note that the χ^2 estimates account for the error inherent to the computation of SIDIS multiplicities arising from varying the input PDFs within their quoted uncertainties.

Even though the nuclear modification of the PDFs for nucleons bound in deuteron targets has been acknowledged to be a non-negligible, percentish-level effect a long time ago [41], most quantitative estimates still suggest a flavor-independent, multiplicative factor that would cancel in the SIDIS multiplicities (except for the small NLO correction stemming from initial-state gluons), and, therefore, we disregard this small correction in our analyses. In any case, the fairly sizable PDF uncertainties can be viewed to cover for this type of uncertainty as well.

We use the standard Mellin technique [5, 42] to precalculate look-up tables for each data point at NLO accuracy to speed up the fitting procedure and to facilitate the uncertainty estimates significantly. We recall that at NLO, the relevant hard scattering coefficient functions for SIDIS [43–45] depend in a non-trivial way on both

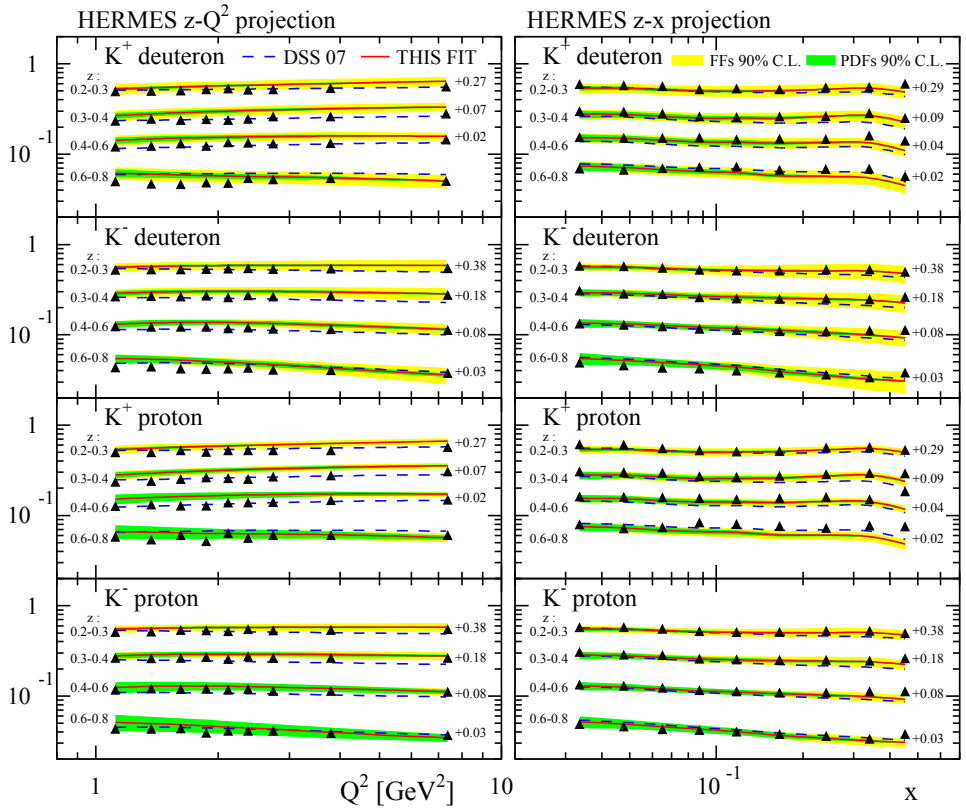

FIG. 5: Comparison of our NLO results (solid lines) for charged kaon multiplicities in SIDIS in four different bins of z with data from the HERMES Collaboration [19] for both proton and deuteron targets. The $z-Q^2$ and $z-x$ projection are shown on the left-hand- and right-hand-side, respectively. The light shaded (yellow) bands correspond to uncertainty estimates at 90% C.L., the dark shaded (green) bands illustrate the PDF uncertainty also at 90% C.L. The results obtained with the DSS 07 set of FFs (dashed lines) are included as well. As indicated in the plot, different constant factors are added to the multiplicities to better distinguish the results for different ranges of z in each panel.

x and z, such that an often used, naive approximation, where the x and the z dependence in Eq. (2) is assumed to completely factorize, is inadequate and bound to fail. Even at LO accuracy such an assumption cannot work as soon as different quark flavors fragment differently into the observed hadron, which they do for charged kaons and all other hadrons.

Before discussing the results, we remark that the use of the HERMES multiplicity data as a means of providing a reliable flavor and charge separation for kaon FFs in the DSS 07 fit was often questioned in the past [46] in rather harsh terms; likewise, for pion FFs. It has even been suggested that the DSS 07 FFs were "inadequate" since they were based on preliminary data, significantly different from the final ones, and, in any case, could not reproduce the multiplicities as a function of x [46]. From Fig. 5 it is evident that *both* HERMES projections, $z-Q^2$ and $z-x$, can be reproduced very well within the estimated uncertainties by the present global fit that also includes the COMPASS SIDIS data which cover a broader range in Q^2; see below. Even the old DSS 07 fit (dashed lines), based on a much reduced set of data and outdated PDFs, nicely reproduces not only the final $z-Q^2$ dependent multiplicities by HERMES but also the $x-z$ dependent ones, not included in the original fit.

In Fig. 5 we also show our uncertainty estimates at 90% C.L. for both the FFs obtained from the fit and the MMHT PDFs computed from the corresponding Hessian sets [9]. It is worth noticing that depending on the charge of the final-state kaon, the type of target, and the kinematics, one or the other source of uncertainty prevails, showing what type of data and kinematics may help to constraint either FFs or PDFs in the future. It also suggests that the averages over charges and/or kinematic bins, that is sometimes applied to the multiplicity data, actually dilutes their constraining power and may potentiate the propagation of uncertainties.

The newly available data from the COMPASS Collaboration [22], taken at a higher c.m.s. energy than the HERMES data, are a very important ingredient for the present analysis as they shed light on the validity of using a standard, leading-twist pQCD framework at NLO accuracy to describe multiplicity data for charged kaons at the comparatively low scales Q^2 reached at HERMES.

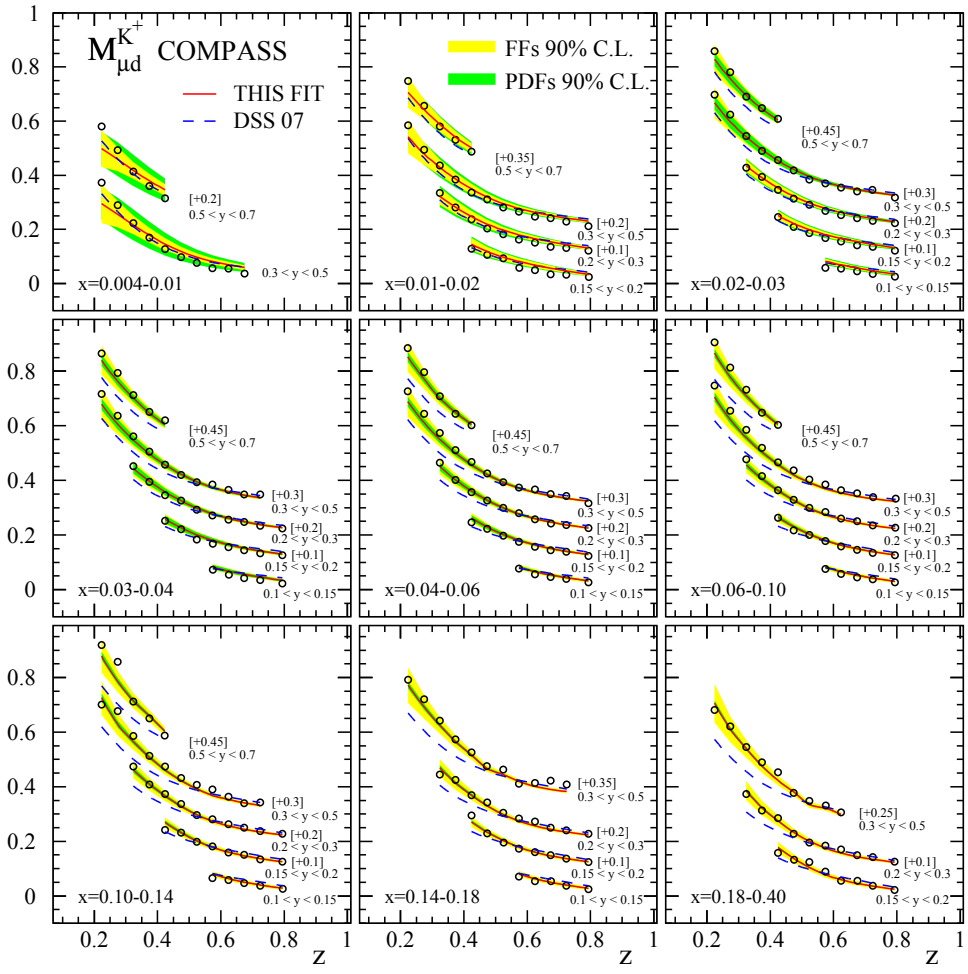

FIG. 6: Comparison of our NLO results for K^+ multiplicities in SIDIS (solid lines) with data from the COMPASS experiment [22] taken on a deuteron target for various bins in x and y. As in Fig. 5, the light (yellow) and dark (green) shaded bands correspond to FF and PDF uncertainty estimates at 90% C.L., respectively. Also shown are the results obtained with our previous DSS 07 set of FFs (dashed lines). As indicated in the plot, different constant factors are added to the multiplicities $M^{K^+}_{\mu d}$ to more easily distinguish the results for different values of y (i.e. Q^2) in the same bin of x.

Achieving a good global fit of data taken at different energies and kinematic ranges with a universal set of parton-to-kaon FFs cannot be taken for granted and provides a non-trivial check for the consistency of different measurements.

More specifically, in the present fit we include the charged kaon results from COMPASS obtained on a deuteron target [22]. The data are presented as a function of z in 9 bins of x, each subdivided into various bins in y that effectively select different Q^2-ranges. In total 309 data points pass our cuts for both K^+ and K^- multiplicities. The comparison of the COMPASS data to the results of our global analysis at NLO accuracy is presented in Figs. 6 and 7. A very satisfactory agreement is achieved in almost all bins across the entire kinematic regime covered by data as can be also inferred from Tab. I; the obtained χ^2/d.o.f. for both K^+ and K^- multiplicities is about 1. As in Fig. 5, the shaded bands illustrate our uncertainty estimates at 90% C.L. for both the FFs and the PDFs.

First and foremost, these results demonstrate that the low-energy HERMES [19] and the new COMPASS [22] charged kaon multiplicity data can be described simultaneously and, equally important, without spoiling the agreement with SIA results discussed before. This is, to a somewhat lesser extent, even the case when one adopts the old DSS 07 set of kaon FFs. As can be seen from Figs. 6 and 7, they lead to a fair agreement with the COMPASS data without any re-fitting except for some of the bins corresponding to the highest Q^2 values; for the $z-Q^2$ projections of the HERMES data, shown in the left panel of Fig. 5, the DSS 07 FFs even lead to a slightly better description of the data than the new, updated global fit. The bottom line is, that the new COMPASS data

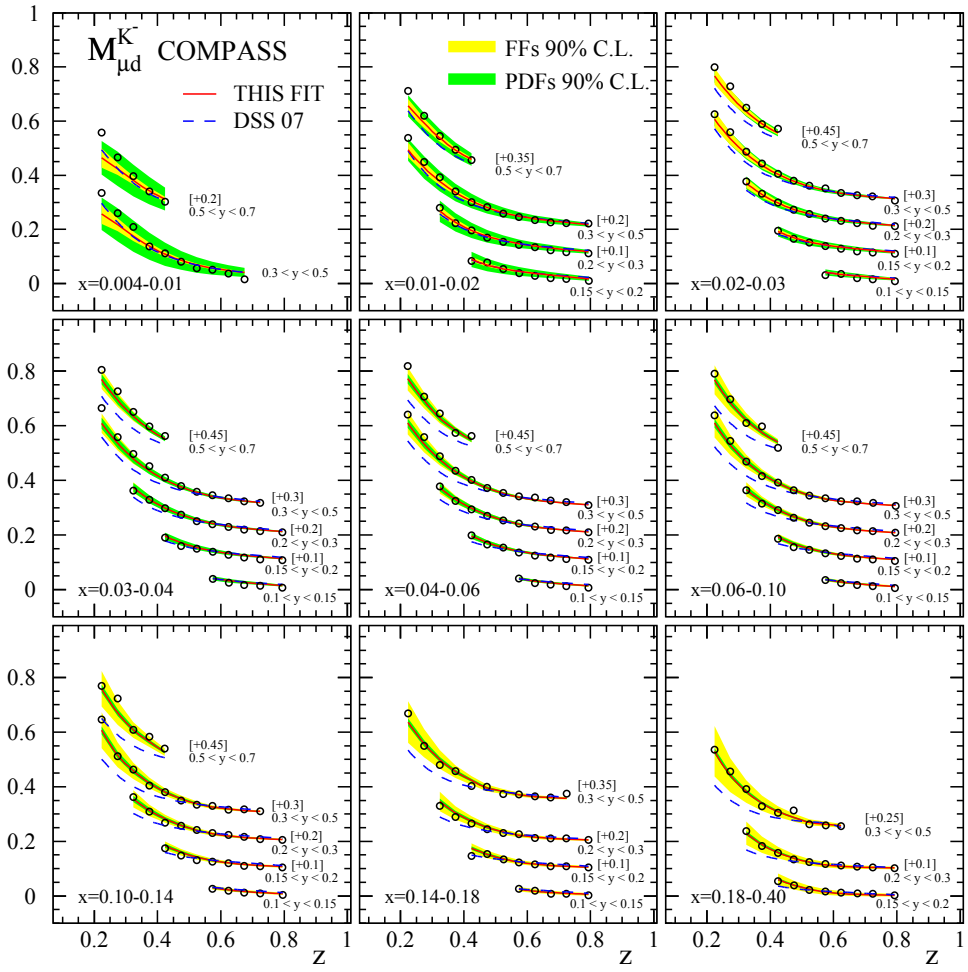

FIG. 7: Same as in Fig. 6 but now for the K^- multiplicities $M^{K^-}_{\mu d}$.

mainly correct the charge and flavor separation provided by the DSS 07 set of FFs at higher Q^2 values, an information that was beyond the reach of the HERMES data adopted in the DSS 07 fit.

We end the discussion of the SIDIS data by noticing that the χ^2/d.o.f. values obtained for some of the HERMES data, in particular, for K^+ multiplicities on a proton target, are higher than for COMPASS. While such fluctuations in χ^2 are perfectly normal in a global QCD analysis of a large amount of data sets, we believe that there is further room for improvement by exploring in more detail the interplay of the used set of PDFs with the quality of the fit to SIDIS data. None of the available sets of PDFs is constrained by data in most of the kinematic regime accessible at HERMES, mainly because stringent cuts on Q^2 are applied in these fits. Hence, it might be very worthwhile to perform a combined, i.e., simultaneous, global analysis of FFs and PDFs in the future, a task which is, however, well beyond the scope of this paper. A first attempt in this direction will be made in a forthcoming publication [47].

D. RHIC and LHC Data

The third and final main ingredient in our global analysis of parton-to-kaon FFs is the experimental information coming from hadron-hadron collisions, more specifically, single-inclusive high-p_T kaon production in pp collisions at BNL-RHIC and the CERN-LHC. Compared to the original DSS 07 analysis [3], which made use of the BRAHMS data for charged kaons and STAR results for K^0_S production at mid rapidities, both sets are limited to very low values of transverse momentum ($p_T < 5\,\text{GeV}$), we can now utilize new results from the STAR Collaboration for charged kaons $K^\pm$ [24] up to $p_T \simeq 13\,\text{GeV}$ as well as first data from the ALICE Collaboration at LHC energies [23].

Due to the complexity of the underlying hard-scattering processes at NLO accuracy [48], the repeated numerical evaluation of single-inclusive hadron production yields in pp collisions in a χ^2-minimization procedure is very time-consuming. The use of a fast, grid-based method to implement the relevant NLO expressions effi-

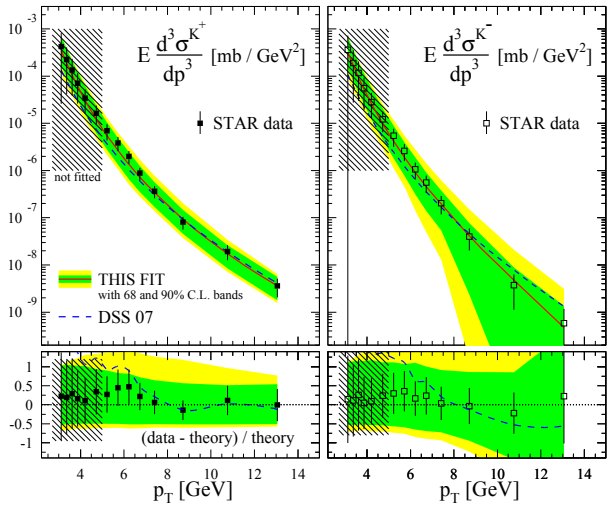

FIG. 8: Comparison of our NLO results for the K^+ (left-hand-side) and K^- (right-hand-side) cross sections in pp collisions at $\sqrt{S} = 200\,\text{GeV}$ and mid rapidity with the STAR data [24]. The inner and outer shaded bands correspond to uncertainty estimates at 68% and 90% C.L., respectively. Also shown are the results obtained with the DSS 07 set of kaon FFs (dashed lines). The lower panels show the corresponding results for (data-theory)/theory.

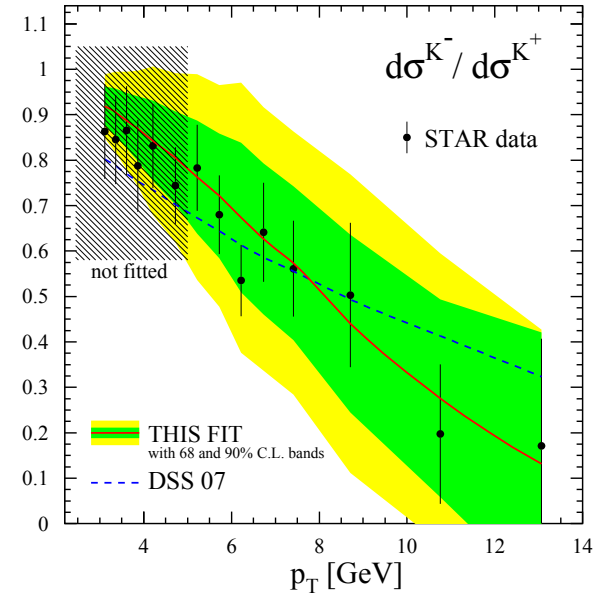

FIG. 9: Same as in Fig. 8 but now for the K^-/K^+ cross section ratio.

ciently and without the need of any approximations such as "K-factors" is indispensable here. As in all our various previous global analyses [3, 5, 27, 28], and for the implementation of the SIDIS multiplicities in Sec. III C, we resort to the well-tested method based on Mellin moments, see Ref. [42].

Data for inclusive particle spectra at not too large values of p_T in pp collisions draw their relevance in a global fit from the dominance of gluon-induced processes. Many of the observed hadrons stem from the hadronization of gluons both at RHIC and LHC energies [49]. Hence, such data are expected to provide invaluable information on the otherwise (i.e., by SIA and SIDIS data) only weakly constrained gluon FF $D_g^{K^+}$.

In our corresponding global analysis of parton-to-pion FFs in Ref. [15] we have found some tension between the p_T spectra of neutral pions measured at $\sqrt{S} = 200\,\text{GeV}$ at RHIC and results from the LHC at much higher c.m.s. energies up to $\sqrt{S} = 7\,\text{TeV}$. In some sense this was already anticipated by comparisons of LHC data to expectations computed with the previous DSS 07 sets of FFs [3, 27], which are known to describe the RHIC data nicely down to, perhaps unexpectedly small $p_T \simeq 1.5\,\text{GeV}$ [3] but were found to grossly overshoot yields for both neutral pions and unidentified charged hadrons (that are dominated by pions) at essentially all p_T values [50]. In particular, at smallish p_T values, below about 5 GeV, the data from RHIC and the LHC appear to be mutually exclusive in a global QCD analysis. Since the origin of this discrepancy could not be traced and we did not want to remove arbitrarily either of the data sets from the analysis, a cut $p_T \geq 5\,\text{GeV}$ was introduced in our fit to remedy the tension, see Ref. [15]. Since we wish to analyze data for the kaon-to-pion ratio, utilizing the latest DSS 14 pion FFs, we decided to proceed with the same cut on p_T in the present analysis of kaon FFs.

Figure 8 shows the data from the STAR Collaboration [24] for single-inclusive charged kaon yields at mid rapidity compared to the results of our fit at NLO accuracy. In Fig. 9 the corresponding cross section ratio is displayed. Since theoretical scale and PDF ambiguities partially cancel in the K^-/K^+ ratio, we decided to use it our fit along with the cross section data for K^+ in the left panel of Fig. 8. To avoid double counting of the same data in the fit, we discard the K^- cross section in the χ^2-minimization but illustrate how well the data are described in the right-hand-side of Fig. 8. As can be seen from both figures and Tab. I, the quality of the fit is very good, even when extrapolated to the p_T-region below 5 GeV. The latter feature indicates that unlike for pions [15] there is considerably less tension with the LHC data from the ALICE Collaboration; see below. Calculations based on the old DSS 07 set of FFs provide a fair description of the STAR charged kaon data but the p_T slope is somewhat off.

Finally, in Fig. 10 we show the charged kaon to charged pion cross section ratio as a function of the transverse momentum p_T as measured by the ALICE Collaboration in pp collisions at mid rapidity at a c.m.s. energy $\sqrt{S}$ of 2.76 TeV [23]. The ratio is estimated by dividing the cross section computed with the parton-to-kaon fragmentation functions obtained in the present analysis by the one obtained with the DSS 14 set of parton-to-pion FFs of Ref. [15], including the quoted normalization shift for the

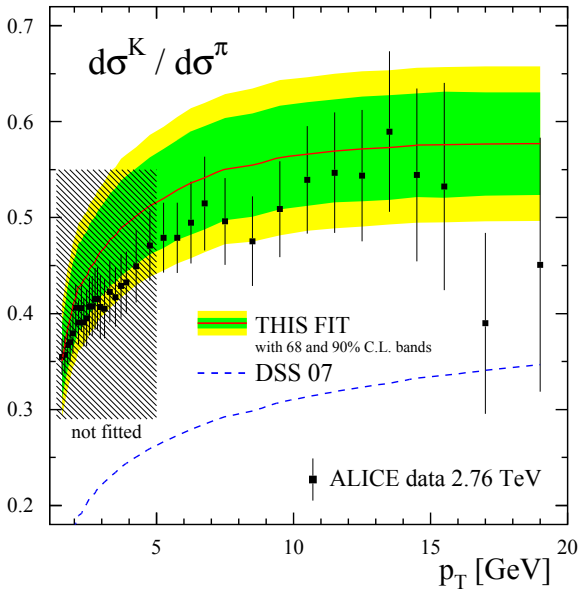

FIG. 10: Ratio of the charged kaon to charged pion cross section at $\sqrt{S} = 2.76$ TeV as measured by ALICE [23] compared to our NLO results (solid line). The pion cross section is computed with the DSS 14 set [15]. The dashed line illustrates the result obtained with the old DSS 07 sets of FFs for both pions and kaons. The inner and outer shaded bands correspond to uncertainty estimates at 68% and 90% C.L., respectively.

ALICE pion data. As can be seen, the current description of the data is much better than the one achieved by the previous DSS 07 sets of pion and kaon FFs (dashed line) which turns out to be way to small in the entire range of p_T. One reason is the much reduced gluon-to-pion FF in the DSS 14 set [15] as compared to DSS 07, which pushes the kaon-to-pion ratio up. In addition, the new fit has a larger gluon-to-kaon FF than in our previous DSS 07 analysis as can be inferred from Fig. 1.

The inner and outer shaded bands in Figs. 8 - 10 represent our uncertainty estimates at 68% and 90% C.L., respectively. The bands are considerably wider than for the corresponding kinematics for pion yields, see Figs. 9-11 in Ref. [15]. In addition, there are theoretical uncertainties from the choice of the factorization and renormalization scales and the set of PDFs in the cross section calculations. For the results shown in the figures, we use a common scale $\mu_f = \mu_r = p_T$ and, as for SIDIS multiplicities, the MMHT set of PDF [9]. Since the relevant kinematics and the dominance of gluons is very similar to the case of single-inclusive pion production at RHIC and the LHC, also the scale and PDF uncertainties for kaons are similar, see Figs. 9-11 in Ref. [15] for estimates. For kaons, however, the uncertainty estimates at 68% and 90% C.L. shown in Figs. 8 - 10 are now the dominant ones, which basically reflects the fact that the experimental data for kaon production is less accurate that those for pions.

IV. SUMMARY AND OUTLOOK

We have presented a new, comprehensive global QCD analysis of parton-to-kaon fragmentation functions at next-to-leading order accuracy including the latest experimental information. The analyzed data comprise single-inclusive kaon production in semi-inclusive electron-positron annihilation, deep-inelastic scattering, and proton-proton collisions and span energy scales ranging from about 1 GeV up to the mass of the Z boson. The very satisfactory and simultaneous description of all data sets within the estimated uncertainties strongly supports the validity of the underlying theoretical framework based on pQCD and, in particular, the notion of factorization and universality for parton-to-kaon fragmentation functions.

Compared to our previous analysis of kaon fragmentation functions in 2007, which was based on much less precise and copious experimental inputs, and to which we have made extensive comparisons throughout this work, we now obtained a significantly better fit, as measured in terms its the global χ^2, using the same functional form as before with only a few additional fit parameters. While most of the favored and unfavored quark-to-kaon fragmentation functions are by and large similar to our previous results, perhaps the most noteworthy change is a larger gluon-to-kaon fragmentation function, which can be tested and constrained further by upcoming data from the LHC experiments.

The wealth of new data included in our updated global analysis allow for the first time to perform a reliable estimate of uncertainties for parton-to-kaon fragmentation functions based on the standard iterative Hessian method. The availability of Hessian sets will significantly facilitate the propagation of these uncertainties to other observables with identified kaons. The obtained uncertainties are still sizable in the kinematic regions covered and constrained by data and they quickly deteriorate beyond. They range at best from about twenty to thirty percent for the total strange quark fragmentation function and from ten to twenty five percent for the total u quark and the gluon fragmentation functions. Another new asset of the current analysis was to analytically determine the optimum normalization shift for each data set in the fit, which greatly facilitated the fitting procedure.

The newly obtained kaon fragmentation functions and their uncertainty estimates will be a crucial ingredient in future global analyses of both helicity and transverse-momentum dependent parton densities, which heavily draw on data with identified kaons in the final-state. Our results will also serve as the baseline in heavy-ion and proton-heavy ion collisions, where one of the main objectives is to quantify and understand possible modifications of hadron production yields by the nuclear medium. Since pions and kaons constitute by far the largest fraction in frequently measured yields of *unidentified* charged hadrons, our newly updated sets of fragmentation func-

tions for both will be a good starting point for a future global QCD analysis of fragmentation functions for unidentified hadrons. It will be interesting to quantify how much room is left for other hadron species, in particular, for protons.

Further improvements of parton-to-kaon fragmentation functions from the theory side should include an improved treatment of heavy quark-to-kaon fragmentation functions, likely along similar lines as for heavy flavor parton densities. Also, the impact of higher order corrections beyond the next-to-leading order accuracy and all-order resummations should be explored. Some results in all these directions have become available recently, however, complete next-to-next-to-leading order corrections are currently only available for an analysis of electron-positron annihilation data. Also the potential bias from the choice of parton distribution functions in the extraction of fragmentation functions from, in particular, semi-inclusive deep-inelastic scattering at not too large scales is worth investigating further. Ultimately, a combined global analysis of parton distribution and fragmentation functions must be the goal.

On the experimental side, the LHC will continue to provide new, valuable data on identified and unidentified hadron spectra. To improve our knowledge on the flavor separation of fragmentation functions, it will be of paramount importance to fully utilize the unprecedented capabilities in semi-inclusive deep-inelastic scattering that will open up at a future electron-ion collider, a project that is currently under scrutiny in the U.S.

Acknowledgments

We are grateful to G. Schnell and E. C. Aschenauer (Hermes), M. Leitgab and R. Seidl (Belle) and F. Kunne, E. Seder (Compass) for helpful discussions about their measurements. We warmly acknowledge vivid discussions with E. Leader about the consistency of SIDIS data. The work of RJHP is partially supported by CONACyT and PROFAPI 2015 grant No. 121. This work was supported in part by CONICET, ANPCyT, and the Institutional Strategy of the University of Tübingen (DFG, ZUK 63).

[1] R. P. Feynman, "Photon-Hadron Interactions", Reading, 1972.
[2] See, e.g., J. C. Collins, D. E. Soper, and G. F. Sterman, Adv. Ser. Direct. High Energy Phys. **5**, 1 (1988).
[3] D. de Florian, R. Sassot, and M. Stratmann, Phys. Rev. D **75**, 114010 (2007).
[4] D. Boer *et al.*, `arXiv:1108.1713 [nucl-th]`; A. Accardi *et al.*, Eur. Phys. J. A **52**, 268 (2016). E. C. Aschenauer *et al.*, `arXiv:1409.1633 [physics.acc-ph]`.
[5] D. de Florian, R. Sassot, M. Stratmann, and W. Vogelsang, Phys. Rev. Lett. **101**, 072001 (2008); Phys. Rev. D **80**, 034030 (2009).
[6] E. C. Aschenauer, R. Sassot, and M. Stratmann, Phys. Rev. D **86**, 054020 (2012); Phys. Rev. D **92**, 094030 (2015).
[7] D. de Florian and R. Sassot, Phys. Rev. D **51**, 6052 (1995).
[8] R. D. Ball *et al.* [NNPDF Collaboration], JHEP **1504**, 040 (2015).
[9] L. A. Harland-Lang, A. D. Martin, P. Motylinski, and R. S. Thorne, Eur. Phys. J. C **75**, 204 (2015).
[10] S. Dulat *et al.*, Phys. Rev. D **93**, 033006 (2016).
[11] S. Kretzer, Phys. Rev. D **62**, 054001 (2000); B. A. Kniehl, G. Kramer, and B. Potter, Nucl. Phys. B **582**, 514 (2000); S. Albino, B. A. Kniehl, and G. Kramer, Nucl. Phys. B **725**, 181 (2005); *ibid.* **803**, 42 (2008); M. Hirai, S. Kumano, T.-H. Nagai, and K. Sudoh, Phys. Rev. D **75**, 094009 (2007); N. Sato, J. J. Ethier, W. Melnitchouk, M. Hirai, S. Kumano, and A. Accardi, Phys. Rev. D **94**, 114004 (2016).
[12] M. Epele, R. Llubaroff, R. Sassot, and M. Stratmann, Phys. Rev. D **86**, 074028 (2012).
[13] See, E. Christova and E. Leader, Phys. Rev. D **94**, 096001 (2016), and references therein for a recent discussion of the subtleties related to including hadron mass corrections.
[14] See, for instance, E. Leader, A. V. Sidorov, and D. B. Stamenov, Phys. Rev. D **91**, 054017 (2015), and references therein.
[15] D. de Florian, R. Sassot, M. Epele, R. J. Hernandez-Pinto, and M. Stratmann, Phys. Rev. D **91**, 014035 (2015).
[16] J. Pumplin, D. R. Stump, and W. K. Tung, Phys. Rev. D **65**, 014011 (2001); J. Pumplin, D. Stump, R. Brock, D. Casey, J. Huston, J. Kalk, H. L. Lai, and W. K. Tung, Phys. Rev. D **65**, 014013 (2001).
[17] J. P. Lees *et al.* [BaBar Collaboration], Phys. Rev. D **88**, 032011 (2013).
[18] M. Leitgab *et al.* [Belle Collaboration], Phys. Rev. Lett. **111**, 062002 (2013).
[19] A. Airapetian *et al.* [Hermes Collaboration], Phys. Rev. D **87**, 074029 (2013).
[20] A. Hillenbrand, "Measurement and Simulation of the Fragmentation Process at HERMES", Ph.D. thesis, Erlangen Univ., Germany, September 2005; private communications.
[21] E. C. Aschenauer *et al.* [HERMES Collaboration], Phys. Rev. D **92**, 098102 (2015).
[22] C. Adolph *et al.* [COMPASS Collaboration], `arXiv:1608.06760 [hep-ex]` (to appear in Phys. Lett. B).
[23] B. Abelev *et al.* [Alice Collaboration], Phys. Lett. B **736**, 196 (2014).
[24] G. Agakishiev *et al.* [Star Collaboration], Phys. Rev. Lett. **108** (2012) 072302.
[25] D. P. Anderle, F. Ringer, and M. Stratmann, Phys. Rev. D **92**, 114017 (2015).
[26] D. P. Anderle, T. Kaufmann, F. Ringer, and M. Strat-

mann, arXiv:1611.03371 [hep-ph].
[27] D. de Florian, R. Sassot, and M. Stratmann, Phys. Rev. D **76**, 074033 (2007).
[28] C. A. Aidala, F. Ellinghaus, R. Sassot, J. P. Seele, and M. Stratmann, Phys. Rev. D **83**, 034002 (2011).
[29] M. Epele, C. A. Garcia Canal, and R. Sassot, Phys. Rev. D **94**, 034037 (2016).
[30] D. Buskulic *et al.* [ALEPH Collaboration], Z. Phys. C **66**, 355 (1995).
[31] P. Abreu *et al.* [DELPHI Collaboration], Eur. Phys. J. C **5**, 585 (1998).
[32] R. Akers *et al.* [OPAL Collaboration], Z. Phys. C **63**, 181 (1994).
[33] K. Abe *et al.* [SLD Collaboration], Phys. Rev. D **59**, 052001 (1999).
[34] G. Abbiendi *et al.* [OPAL Collaboration], Eur. Phys. J. C **16**, 407 (2000).
[35] I. Arsene *et al.* [BRAHMS Collaboration], Phys. Rev. Lett. **98**, 252001 (2007).
[36] B. I. Abelev *et al.* [STAR Collaboration], Phys. Rev. C **75**, 064901 (2007).
[37] H. Aihara *et al.* [TPC/TWO GAMMA Collaboration], Phys. Lett. B **184**, 299 (1987); Phys. Rev. Lett. **61**, 1263 (1988); X. -Q. Lu, Ph.D. thesis, Johns Hopkins University, UMI-87-07273, 1987.
[38] A.D. Martin, R.G. Roberts, W.J. Stirling, and R.S. Thorne, Eur. Phys. J. **C28**, 455 (2003).
[39] A.D. Martin, R.G. Roberts, W.J. Stirling, and R.S. Thorne, Phys. Lett. **B531**, 216 (2002).
[40] M. Cacciari and S. Catani, Nucl. Phys. B **617**, 253 (2001); J. Blumlein and V. Ravindran, Phys. Lett. B **640**, 40 (2006); S. Moch and A. Vogt, Phys. Lett. B **680**, 239 (2009); D. P. Anderle, F. Ringer, and W. Vogelsang, Phys. Rev. D **87**, 034014 (2013).
[41] See, e.g., L. N. Epele, H. Fanchiotti, C. A. Garcia Canal, and R. Sassot, Phys. Lett. B **275**, 155 (1992).
[42] M. Stratmann and W. Vogelsang, Phys. Rev. D **64**, 114007 (2001).
[43] G. Altarelli, R. K. Ellis, G. Martinelli, and S. Y. Pi, Nucl. Phys. B **160**, 301 (1979); W. Furmanski and R. Petronzio, Z. Phys. C **11**, 293 (1982).
[44] D. de Florian, M. Stratmann, and W. Vogelsang, Phys. Rev. D **57**, 5811 (1998).
[45] D. Graudenz, Nucl. Phys. B **432**, 351 (1994); L. Trentadue and G. Veneziano, Phys. Lett. B **323**, 201 (1994); D. de Florian, C. A. Garcia Canal, and R. Sassot, Nucl. Phys. B **470**, 195 (1996).
[46] See, e.g., E. Leader, talk presented at the "22nd International Spin Symposium", Urbana, IL, 2016.
[47] I. Borsa, R. Sassot, and M. Stratmann, work in progress.
[48] F. Aversa, P. Chiappetta, M. Greco, and J. P. Guillet, Nucl. Phys. B **327**, 105 (1989); B. Jager, A. Schafer, M. Stratmann, and W. Vogelsang, Phys. Rev. D **67**, 054005 (2003); D. de Florian, Phys. Rev. D **67**, 054004 (2003).
[49] See, e.g., R. Sassot, M. Stratmann, and P. Zurita, Phys. Rev. D **82**, 074011 (2010).
[50] See, for instance, D. d'Enterria, K. J. Eskola, I. Helenius, and H. Paukkunen, Nucl. Phys. B **883**, 615 (2014).